



**Acoustics'08
Paris**
June 29-July 4, 2008

www.acoustics08-paris.org

euonoise

Regularization method applied to deconvolution problem in Real-Time Acoustic Holography

Sebastien Paillasseur, Jean-Hugh Thomas and Jean-Claude Pascal

ENSIM - LAUM, Université du Maine, rue Aristote, 72085 Le Mans, France
sebastien.paillasseur.etu@univ-lemans.fr

Near-field Acoustic Holography (NAH) is a measuring process for locating stationary sound sources from measurements made by an antenna of microphones positioned near the acoustic source plane. In order to characterize non-stationary sources, a new formulation has been introduced to propagate signals on a forward plane using a convolution product with an impulse response in the time-wavenumber domain. The purpose of this paper is to solve the deconvolution problem related to this formulation and thus to introduce Real-Time Acoustic Holography. Taking the evanescent waves into account improves the spatial resolution of the solution but makes the deconvolution problem "ill-posed". In addition, the sampling of the impulse response is a delicate point. To enhance the source reconstruction several methods based on regularization and processing of the impulse response are experimented on a simulation case involving three non-stationary acoustic monopoles. The results show that low-pass filtering the impulse response and then inverting it using Tikhonov regularization improve the continuous time reconstruction of the back-propagated pressure field.

1 Introduction

The acoustic holography is a measuring process to localize sound sources from measurements made with an array of microphones located in the near-field of the acoustic source plane as shown in Fig.1. This method called Near-field Acoustic Holography (NAH) was introduced in the eighties [1] and is used for stationary sources. In order to characterize non-stationary sources, some methods like Time Domain Holography [2] or Time Method [3] may be used. A new formulation has been introduced [4] to propagate signals on a forward plane $z=z_f$ ($z_f > z_m$) using a convolution product with an impulse response in the time-wavenumber domain. This formulation does not require any assumption about the stationary properties of the sources and can describe the time dependency of the propagated sound pressure field on the forward plane. In this paper we will first present a method to solve the deconvolution problem related to this formulation in order to introduce the Real-Time Nearfield Acoustic Holography and then tests different processing applied on the impulse response to improve the effectiveness of this method.

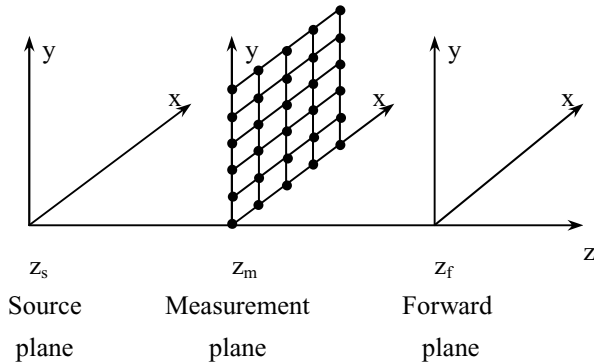


Fig.1 Geometry of Acoustic Holography

2 Forward propagation

The direct problem of the Real-Time Nearfield Acoustic Holography consists in propagating the sound pressure field measured on a plane $z=z_s$ to a forward plane $z=z_f$. It was shown [4] that this problem can be solved by using the convolution product of the time-dependent wavenumber spectrum $P(k_x, k_y, z_m, t)$ with an impulse response h :

$$P(k_x, k_y, z_f, t) = P(k_x, k_y, z_m, t) * h(k_x, k_y, z_f - z_m, t) \quad (1)$$

where k_x and k_y are the wavenumbers along the axis x and y .

The time-dependent wavenumber spectrum $P(k_x, k_y, z, t)$ is calculated by applying a two dimensional Fourier transform along the axis x and y to the sound pressure field $p(x, y, z, t)$:

$$P(k_x, k_y, z, t) = \int_{-\infty}^{+\infty} \int_{-\infty}^{+\infty} p(x, y, z, t) e^{j(k_x x + k_y y)} dx dy \quad (2)$$

The expression of the impulse response h is obtained from the solution of the two dimensional Fourier transform of the wave equation:

$$\frac{\partial^2 P(k_x, k_y, z, t)}{\partial z^2} - \frac{1}{c^2} \frac{\partial^2 P(k_x, k_y, z, t)}{\partial t^2} - (k_x^2 + k_y^2) P(k_x, k_y, z, t) = 0 \quad (3)$$

where c (m.s^{-1}) is the sound velocity in the air. If we note the propagation distance $\Delta z = z_f - z_m$, the wavenumber $k_r = \sqrt{k_x^2 + k_y^2}$, the propagation delay $\tau = \Delta z / c$ and the transition pulsation $\Omega_r = c k_r$, the impulse response h can be written

$$h(\Omega_r, \tau, t) = \delta(t - \tau) - \tau \Omega_r \frac{J_1(\Omega_r \sqrt{t^2 - \tau^2})}{\Omega_r \sqrt{t^2 - \tau^2}} \Gamma(t - \tau), \quad (4)$$

where J_1 is the first order Bessel function, $\delta(t)$, the Dirac delta function and $\Gamma(t)$ the Heaviside function. Replacing the expression of h in the Eq.(1) leads to the time-dependent wavenumber spectrum on the forward plane $P(k_x, k_y, z_f, t)$. It is then possible to calculate the instantaneous spatial pressure in the forward plane $p(x, y, z_f, t)$ by applying the inverse two dimensional Fourier transform to $P(k_x, k_y, z_f, t)$.

3 Backward Propagation

In the case of Real-Time Nearfield Acoustic Holography we are seeking the time-dependent pressure field on the source plane from measurements made by a microphone array in the nearfield of the source plane. In order to back-propagate the pressure field radiated by non-stationary sources it is necessary to solve the deconvolution problem of the Eq.(1) which can be written as:

$$P(k_x, k_y, z_s, t) = P(k_x, k_y, z_m, t) * h^{-1}(k_x, k_y, z_m - z_s, t) \quad (5)$$

In order to explain the backpropagation of the instantaneous wavenumber spectrum of a pair (k_x, k_y) the Fourier transform is applied on the inverse of the impulse response h^{-1} :

$$TF\{h^{-1}(k_x, k_y, \Delta z, t)\} = H^{-1}(f_T, \Delta z, f) = \begin{cases} e^{\frac{2\pi j}{c} \frac{\Delta z}{c} \sqrt{f^2 - f_T^2}} & \text{for } f \geq f_T \\ e^{\frac{2\pi j}{c} \frac{\Delta z}{c} \sqrt{f_T^2 - f^2}} & \text{for } f < f_T \end{cases} \quad (6)$$

where f_T is the transition frequency

$$f_T = \frac{c\sqrt{k_x^2 + k_y^2}}{2\pi} = \frac{\Omega_r}{2\pi}. \quad (7)$$

As shown in Fig.2 the backpropagation acts differently depending on the frequency of the components, however this separation is not possible in the time-wavenumber domain :

The components with a frequency $f \geq f_T$ correspond to the progressive waves. The backpropagation of the progressive waves leads to a change of phase but their amplitudes remain unchanged.

The components with a frequency $f < f_T$ correspond to the evanescent waves. The backpropagation of the evanescent waves leads to an amplification of their amplitudes but their phases remain unchanged. In the presence of measurement noise this amplification may induce erroneous values during the backpropagation. The problem is said "ill-posed" and requires processing with a regularization method.

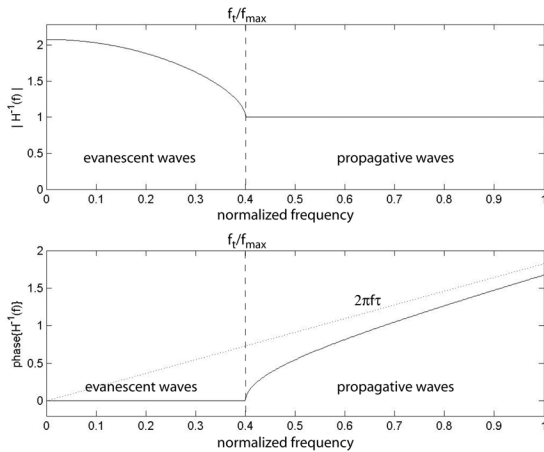


Fig.2 Modulus and phase of the theoretical Fourier transform of the inverse impulse response with $f_{max} = f_e/2$, where f_e is the sampling frequency.

4 Solving the backward propagation

The method we chose to solve this problem is the standard Tikhonov regularization [5] as it does not require any assumption on the processed signal. This method consists in adding a constraint on the solution which is the minimization of its energy. If we consider the linear system

$$\mathbf{h}\mathbf{x} = \mathbf{y} \quad (8)$$

where \mathbf{h} , \mathbf{y} are known and \mathbf{x} is to be calculated, the standard Tikhonov regularized solution \mathbf{x}_λ of Eq.(8) is given by :

$$\mathbf{x}_\lambda = \min \left\{ \|\mathbf{h}\mathbf{x} - \mathbf{y}\|_2^2 + \lambda^2 \|\mathbf{x}\|_2^2 \right\} \quad (9)$$

where $\|\mathbf{x}\|_2$ is the L2 norm of \mathbf{x} and λ is the regularization parameter which will influence the weight of the regularization. This parameter is to be estimated by the use

of methods like the Generalized Crossed Validation (GCV) [6] or the L-curve [7]. First of all it is necessary to discretize and rewrite the convolution product in Eq.(1) into a matrix product equivalent to the linear system in Eq.(8).

If we consider the discretized convolution product

$$y(n) = x(n) * h(n), \quad (10)$$

the Eq.(10) is equivalent to

$$\begin{bmatrix} y(1) \\ y(2) \\ \vdots \\ y(N) \end{bmatrix} = \begin{bmatrix} h(1) & 0 & \cdots & 0 \\ h(2) & \ddots & \ddots & \vdots \\ \vdots & \ddots & \ddots & 0 \\ h(N) & \cdots & h(2) & h(1) \end{bmatrix} \begin{bmatrix} x(1) \\ x(2) \\ \vdots \\ x(N) \end{bmatrix} \quad (11)$$

It is then possible to apply the standard Tikhonov regularization for each pair (k_x, k_y) . The Singular Value Decomposition (SVD) is a mathematical tool used to apply the regularization. The SVD of a matrix \mathbf{h} is

$$\mathbf{h} = \mathbf{U} \mathbf{S} \mathbf{V}^H \quad (12)$$

where \mathbf{S} is the diagonal matrix of the singular values of \mathbf{h} , \mathbf{U} and \mathbf{V} are the singular matrix associated and are orthonormal. \mathbf{V}^H is the transconjugate of the matrix \mathbf{V} . The inverse of \mathbf{h} is

$$\begin{aligned} \mathbf{h}^{-1} &= (\mathbf{U} \mathbf{S} \mathbf{V}^H)^{-1} = \mathbf{V} \mathbf{S}^{-1} \mathbf{U}^H \\ &= \mathbf{V} \text{diag} \left(\frac{1}{s_1}, \dots, \frac{1}{s_N} \right) \mathbf{U}^H \end{aligned} \quad (13)$$

The solution of Eq.(8) can be written as

$$\mathbf{x} = \sum_{i=1}^N \frac{\mathbf{u}_i^H \mathbf{y}}{s_i} \mathbf{v}_i. \quad (14)$$

It has been shown [8] that the regularization will act as a filter on the singular values of \mathbf{h}

$$\mathbf{x}_\lambda = \sum_{i=1}^N f_i \frac{\mathbf{u}_i^H \mathbf{y}}{s_i} \mathbf{v}_i, \quad (15)$$

where \mathbf{x}_λ is the regularized solution and f_i the coefficients of the regularization filter. In the case of the standard Tikhonov regularization, the filter coefficients f_i are

$$f_i = \frac{s_i^2}{s_i^2 + \lambda^2}. \quad (16)$$

To estimate the regularization parameter we used the General Crossed Validation, which consists in minimizing the function G defined by:

$$G \equiv \frac{\|\mathbf{h}\mathbf{x}_\lambda - \mathbf{y}\|_2^2}{(\text{tr}(\mathbf{I} - \mathbf{h}\mathbf{h}_\lambda^{-1}))^2}, \quad (17)$$

where \mathbf{I} is the identity matrix and \mathbf{h}_λ^{-1} is the regularized inverse of \mathbf{h}

$$\mathbf{x}_\lambda \equiv \mathbf{h}_\lambda^{-1} \mathbf{y}. \quad (18)$$

Once the regularization parameter λ is determined, the regularized solution is given by Eq.(15) where the filter coefficient are calculated with Eq.(16). The method presented in this section is used to solve the inverse problem related to Eq.(1) yielding the backpropagated time-dependent wavenumber spectrum on the source plane.

5 Processing of the impulse response

It has been shown [9] that the direct sampling of the impulse response may leads to distortion even if the sampling rate is relatively high. This is due to the fact that the impulse response is defined by an analytical formulation and thus have an infinite frequency band. Oversampling the impulse response may reduce these distortions but as shown in Fig.3 the impulse response obtained is not satisfactory. In this section we introduce different processing applied to the impulse response in order to remove these distortions. If we note

$$h(\Omega_r, \tau, t) = \delta(t - \tau) - g(\Omega_r, \tau, t) \quad (19)$$

which is derived from Eq.(4), where

$$g(\Omega_r, \tau, t) = \tau \Omega_r^2 \frac{J_1(\Omega_r \sqrt{t^2 - \tau^2})}{\Omega_r \sqrt{t^2 - \tau^2}} \Gamma(t - \tau). \quad (20)$$

Instead of using $g[n]$, the direct sampling of $g(t)$ at the time $t = n\Delta t$, it is possible to use the mean value $\bar{g}[n]$ computed into an interval Δt centered at $t = n\Delta t$

$$\bar{g}[n] = \frac{1}{\Delta t} \int_{n\Delta t - \Delta t/2}^{n\Delta t + \Delta t/2} g(t) dt. \quad (21)$$

The integral in Eq.(21) is approximated by the trapezoidal formula.

Another processing consists in increasing the sampling rate of the impulse response by a factor D yielding a new sampling frequency $f_e' = Df_e$. Thus the impulse response is calculated on $D \times N$ samples and then decimated by a factor D so the sampling frequency f_e'/D matches f_e . This processing involves a low-pass filter on the upsampling impulse response before applying the decimation. Two filters have been experimented, a Chebyshev filter and a Kaiser-Bessel window associated with a cardinal sine defined by

$$w(t) = \tau \Omega_r^2 \frac{I_0\left(\beta \sqrt{1 - (2t/T)^2}\right) \sin(\alpha \pi t f_e)}{I_0(\beta) \pi t} \quad (22)$$

where I_0 is the modified Bessel function of the first kind and order 0. T is the duration of the Kaiser-Bessel window. α is linked to the cut-off frequency of the low-pass filter and β is the parameter which sets the sidelobes of the window. The low-pass filter is applied to the impulse response using convolution yielding the filtered impulse response $g_f(t)$ which can be implemented by using the discrete sum

$$g_f[n] = \sum_m w[m] g[n - m], \quad (23)$$

or by using the numerical approximation of the following integral given by the trapezoidal method

$$g_f(t) = \int_{-T/2}^{+T/2} g(\theta) w(t - \theta) d\theta. \quad (24)$$

Another method to build the impulse response is based on the Fourier transform of the Eq.(1) yielding

$$P(k_x, k_y, z_f, \omega) = P(k_x, k_y, z_m, \omega) H(\Omega_r, \tau, \omega) \quad (25)$$

Eq.(25) is equivalent to the relation between the known pressure field on a plane $z = z_m$ and the pressure on a plane

$z = z_f$ when the studied stationary acoustic sources are confined on the half plane $z \leq z_s$.

$$P(k_x, k_y, z_f, \omega) = P(k_x, k_y, z_m, \omega) G_p(k_r, \Delta z, \omega), \quad (26)$$

where G_p is the propagator defined by

$$G(k_r, \Delta z, \omega) = \begin{cases} e^{-j\Delta z \sqrt{\left(\frac{\omega}{c}\right)^2 - k_r^2}} & \text{for } \omega/c \geq k_r \\ e^{-\Delta z \sqrt{k_r^2 - \left(\frac{\omega}{c}\right)^2}} & \text{for } \omega/c < k_r \end{cases}. \quad (27)$$

Comparing Eq.(25) and Eq.(26) allows us to estimate the frequency response $H(\Omega_r, \tau, \omega)$ as

$$H(\Omega_r, \tau, \omega) = G(k_r, \Delta z, \omega) = \begin{cases} e^{-j\tau \sqrt{\omega^2 - \Omega_r^2}} & \text{for } \omega \geq \Omega_r \\ e^{-\tau \sqrt{\Omega_r^2 - \omega^2}} & \text{for } \omega < \Omega_r \end{cases}. \quad (28)$$

The impulse response is finally obtained by applying an inverse Fourier transform to the frequency response $H(\Omega_r, \tau, \omega)$.

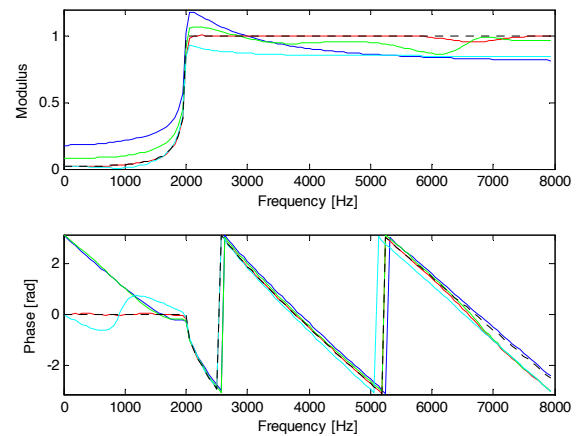


Fig.3 Modulus and phase of the transfer functions $H(\Omega_r, \tau, \omega)$ computed with oversampling method (blue), the average method (cyan), the Chebyshev filtering (green), the numerical Kaiser method (red) and from Eq.(19) (----).

6 Numerical results

6.1 Setup

The setup of the numerical simulations is shown Fig.4. The source plane positionned at $z_s = 0\text{m}$ is composed of three monopoles at the positions $S_1(0.3\text{m}, 0.4\text{m}, 0\text{m})$, $S_2(0.7\text{m}, 0.7\text{m}, 0\text{m})$ and $S_3(0.3\text{m}, 0.7\text{m}, 0\text{m})$. S_1 and S_2 generate a signal with a linear frequency modulation and a gaussian amplitude modulation. S_3 radiates a Morlet wavelet defined by

$$S_3(t) = \cos(2\pi ft) e^{-t^2/2}. \quad (29)$$

These sources have been chosen because of their non-stationnary properties.

The first step consists in simulating the pressure $p_r(x, y, z_m, t)$ acquired by a 11×11 microphone array on the measurement plane $z_m = 0.0215\text{m}$. This pressure will be considered as the reference pressure. The second step is to use the forward propagation presented in Section 1 associated with the

different processing of the impulse response introduced in Section 5 to obtain the pressure on the forward plane $z_f=0.0860\text{m}$. Finally the back-propagation combined with the standard Tikhonov regularization as shown in Section 4 is used to calculate the pressure $p(x,y,z_m,t)$ with $\Delta z=0.0645\text{m}$. The emitted and calculated signals are sampled at a frequency rate $f_e=16000\text{Hz}$ giving 256 samples.

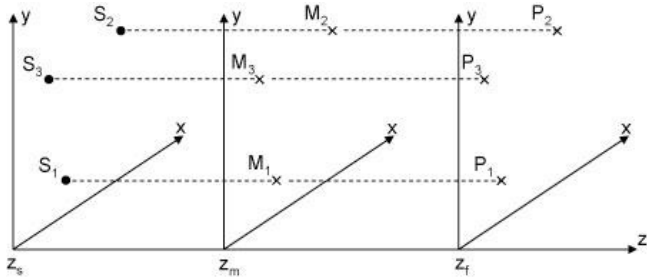


Fig.4 Geometry of the numerical simulations.

6.2 Indicators

In order to compare the effectiveness of the different processing applied to the impulse response we used two temporal indicators T_1 and T_2 defined by

$$T_1 = \frac{\langle p_r(x,y,z_m,t) p(x,y,z_m,t) \rangle}{\sqrt{\langle p_r^2(x,y,z_m,t) \rangle \langle p^2(x,y,z_m,t) \rangle}}, \quad (30)$$

$$T_2 = \sqrt{\frac{\langle p^2(x,y,z_m,t) \rangle}{\langle p_r^2(x,y,z_m,t) \rangle}}, \quad (31)$$

where $\langle \rangle$ is the mean value, $p_r(x,y,z_m,t)$ is the reference time-dependent pressure and $p(x,y,z_m,t)$ is the time-dependent pressure calculated by the back-propagation. T_1 is a correlation coefficient which is sensitive to the similarity between the shapes of the signals and thus between their phase difference. T_2 is the ratio between two root square mean values to characterize the similarity of the amplitudes of both signals.

6.3 Results

The values of the indicators T_1 and T_2 for the three locations M_1 , M_2 and M_3 are summarized in Table 1. The processing used in these simulations involving regularization are the following:

- D is the direct sampling of the impulse response $f_e=16000\text{Hz}$.
- O is the oversampling of the impulse response with a sampling rate frequency $f_e=64000\text{Hz}$.
- A is the average method using the mean value $\bar{g}[n]$ according to Eq.(21).
- C is the decimate method with a factor $D=8$ combined with a Chebyshev low-pass filter.
- K is the low-pass filtering using the Kaiser-Bessel filter with a cut-off frequency $f_c=6640\text{Hz}$ and an upsampling factor $D=2$.

- F is the impulse response obtained by applying an inverse Fourier transform on the frequency response $H(\Omega_r, \tau, \omega)$ defined in Eq.(28).

	M_1					
	D	O	A	C	K	F
T_1	0,670	0,888	0,982	0,995	0,995	0,996
T_2	1,124	0,968	1,125	1,134	1,144	1,143
	M_2					
	D	O	A	C	K	F
T_1	0,678	0,903	0,975	0,996	0,991	0,993
T_2	1,115	0,971	1,114	1,124	1,131	1,131
	M_3					
	D	O	A	C	K	F
T_1	0,629	0,859	0,994	0,992	0,999	0,999
T_2	1,040	0,902	1,094	1,082	1,104	1,103

Table 1 Indicators T_1 and T_2 at the three different locations M_1 , M_2 and M_3 .

The comparisons between the reconstructed temporal pressure signals obtained with the direct sampling of the impulse response (in blue) and the filtering of the impulse response with a low-pass Kaiser-Bessel filter (in black) versus the reference signal (in red) are shown in Fig.5, Fig.6 and Fig.7 at the three different locations M_1 , M_2 and M_3 .

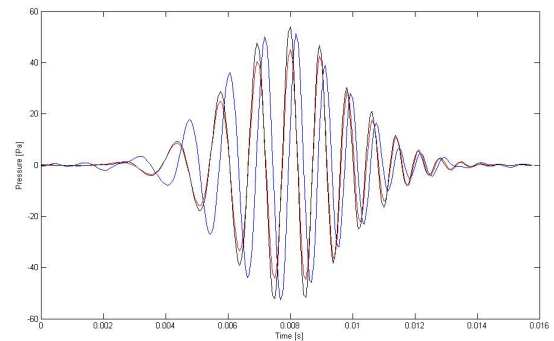


Fig.5 Reconstructed temporal pressure signals obtained with method D (in blue) and with method K (in black) versus the reference signal (in red) for location M_1 .

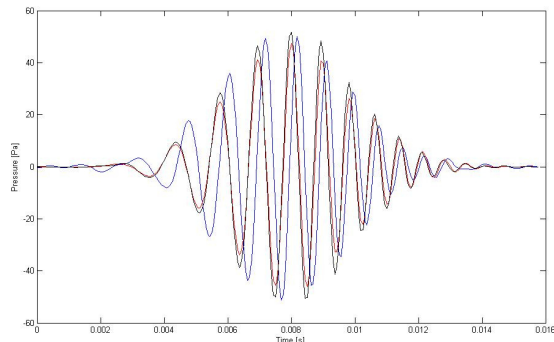


Fig.6 Reconstructed temporal pressure signals obtained with method D (in blue) and with method K (in black) versus the reference signal (in red) for location M_2 .

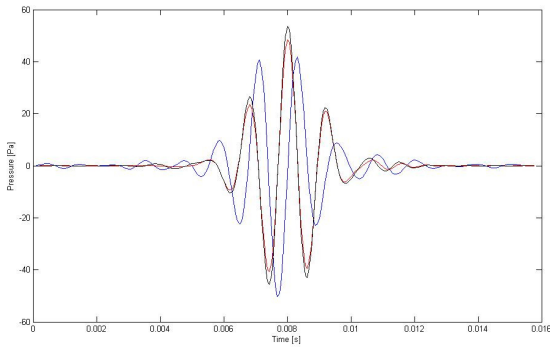


Fig.7 Reconstructed temporal pressure signals obtained with method D (in blue) and with method K (in black) versus the reference signal (in red) for location M_3 .

7 Conclusion

The deconvolution problem related to Real-Time Nearfield Acoustic Holography is an “ill-posed” problem and thus requires specialized processing. An effective method to solve this problem have been introduced in this paper using the standard Tikhonov regularization combined with the General Crossed Validation (GCV). We then introduced different methods to reduce the distortions introduced by sampling the impulse response. We have shown that filtering the impulse response with a Kaiser-Bessel low-pass filter or using the inverse Fourier transform of the frequency response $H(\Omega, \tau, \omega)$ give accurate results in the case of Real-Time Acoustic Holography.

References

- [1] Williams E.G., Maynard J.D. and Skudrzyk E., “Sound source reconstructions using a microphone array”, *J. Acoust. Soc. Am.*, **68**, 340-344 (1980).
- [2] Hald J., “Time domain acoustical holography”, Inter-noise 1995, Newport Beach, 10-12 July 1995, 1349-1354.
- [3] Deblauwe F., Leuridan J., Chauray J.L. and Béguet B., “Acoustic holography in transient conditions”, Sixth International Congress on Sound and Vibration, Copenhagen, 5-8 July 1999, 899-906.
- [4] Grulier V., Thomas J.-H., Pascal J.-C. and Le Roux J.-C., “Time varying forward projection using wavenumber formulation”, Inter-noise 2004, Prague, 22-25 August 2004.
- [5] Williams E.G., “Regularization methods for near-field acoustical holography”, *J. Acoust. Soc. Am.*, **110**, 1976-1988 (2001).
- [6] Iqbal M., “Deconvolution and regularization for numerical solutions of incorrectly posed problems”, *Journal of computational and applied mathematics*, **151**, 463-476 (2001).
- [7] Hansen P.C. and O’Leary D.P., “The use of the L-curve in the regularization of discrete ill-posed problems”, *SIAM J. Sci. Comput.*, **14**, 1487-1503 (1993).
- [8] Jacquelin E., Bennani A. and Hamelin P., “Force reconstruction: analysis and regularization of a deconvolution problem”, *Journal of Sound and Vibration* **265**, 81-107 (2003).
- [9] Grulier V., “Propagation directe et inverse dans l’espace temps-nombre d’onde: Application à une méthode d’holographie acoustique de champ proche pour les sources non-stationnaires”. PhD thesis, Université du Maine, 2005.